

Truncated and Full-Length Thioredoxin-1 Have Opposing Activating and Inhibitory Properties for Human Complement with Relevance to Endothelial Surfaces

This information is current as of March 6, 2022.

Ben C. King, Justyna Nowakowska, Christian M. Karsten, Jörg Köhl, Erik Renström and Anna M. Blom

J Immunol 2012; 188:4103-4112; Prepublished online 19 March 2012;
doi: 10.4049/jimmunol.1101295
<http://www.jimmunol.org/content/188/8/4103>

References This article **cites 54 articles**, 30 of which you can access for free at:
<http://www.jimmunol.org/content/188/8/4103.full#ref-list-1>

Why *The JI*? Submit online.

- **Rapid Reviews! 30 days*** from submission to initial decision
- **No Triage!** Every submission reviewed by practicing scientists
- **Fast Publication!** 4 weeks from acceptance to publication

**average*

Subscription Information about subscribing to *The Journal of Immunology* is online at:
<http://jimmunol.org/subscription>

Permissions Submit copyright permission requests at:
<http://www.aai.org/About/Publications/JI/copyright.html>

Email Alerts Receive free email-alerts when new articles cite this article. Sign up at:
<http://jimmunol.org/alerts>



Truncated and Full-Length Thioredoxin-1 Have Opposing Activating and Inhibitory Properties for Human Complement with Relevance to Endothelial Surfaces

Ben C. King,* Justyna Nowakowska,* Christian M. Karsten,[†] Jörg Köhl,^{†,‡} Erik Renström,[§] and Anna M. Blom*

Thioredoxin (Trx)-1 is a small, ubiquitously expressed redox-active protein with known important cytosolic functions. However, Trx1 is also upregulated in response to various stress stimuli, is found both at the cell surface and secreted into plasma, and has known anti-inflammatory and antiapoptotic properties. Previous animal studies have demonstrated that exogenous Trx1 delivery can have therapeutic effects in a number of disease models and have implicated an interaction of Trx1 with the complement system. We found that Trx1 is expressed in a redox-active form at the surface of HUVEC and acts as an inhibitor of complement deposition in a manner dependent on its Cys-Gly-Pro-Cys active site. Inhibition occurred at the point of the C5 convertase of complement, regulating production of C5a and the membrane attack complex. A truncated form of Trx1 also exists in vivo, Trx80, which has separate nonoverlapping functions compared with the full-length Trx1. We found that Trx80 activates the classical and alternative pathways of complement activation, leading to C5a production, but the inflammatory potential of this was also limited by the binding of inhibitors C4b-binding protein and factor H. This study adds a further role to the known anti-inflammatory properties of Trx1 and highlights the difference in function between the full-length and truncated forms. *The Journal of Immunology*, 2012, 188: 4103–4112.

Thioredoxin (Trx)-1 is a ubiquitously expressed protein, with roles in controlling intracellular redox potential (1). It has disulfide reductase activity, with two cysteine residues (C32 and C35) in its conserved active site being required for this function. Trx1 is also secreted from cells via a signal peptide- and Golgi-independent pathway (2) and is found at elevated levels in the blood of patients in a wide number of disease states, especially so in severe sepsis (3). As such, it is thought to be a marker of oxidative stress. Trx1 also exists in vivo in a truncated form, Trx80. Trx80 has very different properties from the full-length protein, lacking the disulfide reductase activity of the full-length

species, and instead having proinflammatory cytokine-like effects on immune cells (4, 5).

Exogenously administered Trx1 has been shown to inhibit neutrophil chemotaxis (6) as well as prolonging survival and limiting pathology in animal models of ischemia reperfusion (7–10) and sepsis (3), conditions in which complement is known to play a pathogenic role (11, 12). One study also showed that transgenic overexpression, or injection of recombinant Trx1, protects mice from choroidal neovascularisation in a laser-burn model of age-related macular degeneration (13), a disease for which the strongest genetic link is a polymorphism in the complement inhibitor, factor H (14). The therapeutic effect of Trx1 was found to involve interaction with factor H and inhibition of complement activation and leukocyte infiltration (13).

The complement system is an evolutionarily ancient part of the innate immune system, consisting of serum pattern recognition molecules, which then activate further serum complement proteins in an enzymatic cascade (15). Although it is most well-known for its role in attacking pathogens via deposition of opsonins and the lytic membrane attack complex (MAC) C5b-9, complement also plays a role as a danger-sensing system (16) and is able to alert cells of both the innate and adaptive immune system via cell surface receptors for complement proteins and activation products, most notably by production of the anaphylatoxins C3a and C5a. Complement inhibitors are currently under investigation as potential therapeutics in many disease types (17), and further understanding of complement inhibitors is therefore important for future progress.

Because of the previously reported therapeutic role of Trx1 in the choroidal vascularization model (13) and the link between complement activation and neovascularization (18), we further investigated the interactions between Trx1 and complement to clarify its inhibitory properties and possible therapeutic applications. We found that Trx1 inhibits complement activation at the stage of C5

*Section of Medical Protein Chemistry, Department of Laboratory Medicine, Lund University, S-205 02 Malmö, Sweden; [†]Institute for Systemic Inflammation Research, University of Lübeck, 23538 Lübeck, Germany; [‡]Division of Molecular Immunology, Cincinnati Children's Hospital Medical Center, University of Cincinnati College of Medicine, Cincinnati, OH 45229; and [§]Department of Clinical Sciences, Lund University Diabetes Centre, Lund University, S-205 02 Malmö, Sweden

Received for publication May 5, 2011. Accepted for publication February 14, 2012.

This work was supported by the Swedish Research Council (K2009-68X-14928-06-3), the Swedish Foundation for Strategic Research, Cancerfonden, and the Foundations of Österlund, Greta and Johan Kock, Knut and Alice Wallenberg, and Inga-Britt and Arne Lundberg, the Deutsche Forschungsgemeinschaft Research Training Group project (GRK 1727), as well as grants for clinical research from the University Hospital in Malmö and the Region Skåne.

Address correspondence and reprint requests to Prof. Anna M. Blom, Section of Medical Protein Chemistry, Department of Laboratory Medicine, Lund University, Skåne University Hospital, S-205 02 Malmö, Sweden. E-mail address: Anna.Blom@med.lu.se

Abbreviations used in this article: bIAA, iodoacetyl-PEG₂-biotin; bNHS, succinimidobiotin; C5aRA, C5a receptor antagonist; C4BP, C4b binding protein; hiNHS, heat-inactivated normal human serum; MAC, membrane attack complex; MBL, mannose-binding lectin; NHS, normal human serum; OPD, *o*-phenylenediamine dihydrochloride; PDI, protein disulfide isomerase; RPA, reverse passive Arthus; Trx, thioredoxin.

Copyright © 2012 by The American Association of Immunologists, Inc. 0022-1767/12/\$16.00

convertase and MAC formation, and that exogenously applied Trx1 can act to prevent C5a production and deposition of the lytic MAC. In comparison, Trx80 causes activation of complement via the classical and alternative pathways, resulting in production of C5a, but limited amounts of MAC, because of interaction with complement inhibitors factor H and C4b-binding protein (C4BP).

Materials and Methods

Human serum and plasma

Normal human serum (NHS) was pooled from several healthy volunteers with informed consent and under ethical permit of ethical committee of Lund University. Blood was allowed to clot for 20 min at room temperature and for an additional hour on ice. The blood was then spun at $800 \times g$ at 4°C in a precooled centrifuge, and the serum was pooled and frozen in aliquots at -80°C . For C5a chemotaxis assays, plasma was used, because serum contains C5a and C5adesArg produced during blood coagulation (19). Blood was collected with $50 \mu\text{g/ml}$ Repludin (Pharmion), a recombinant hirudin anticoagulant that does not affect complement activation (20), spun at 2000 rpm for 10 min, and the plasma was stored in aliquots at -80°C .

Cells, Abs, and proteins

HUVEC were obtained from Invitrogen and grown in M200 media supplemented with low serum growth supplement (Invitrogen). The cells were used for experiments between passages 1 and 5. Neutrophils were purified from peripheral blood using subsequent Histopaque 1119 (Sigma-Aldrich) and Percoll density centrifugation steps, and purity was assessed by flow cytometry with anti-CD16 staining (Immunotools). Abs used include goat polyclonal ATRX04 (IMCO), specific anti-complement component Abs were purchased from Quidel with the exception of anti-C1q, anti-C4c, and anti-C3d (all from DakoCytomation), goat anti-C9 and rabbit anti-C5b-9 neoepitope (both from Complement Technology), goat anti-mannose-binding lectin (MBL) (R&D Systems), anti-C3/C3a (Hycult), and mouse anti-C4BP (clone MK104, in-house). Mouse monoclonals against ficolins 2 and 3 (I- and H-ficolin) were characterized previously (21, 22) and supplied by Prof. P. Garred (University of Copenhagen, Copenhagen, Denmark). HRP-conjugated secondary Abs were from DakoCytomation. Rabbit serum against Trx1 was generated by Agrisera Ab after vaccination with CFA and recombinant human Trx1, and anti-Trx1 F(ab)₂ was produced by pepsin digestion of affinity purified anti-Trx1 Ab from rabbit anti-Trx1 serum (23). Remaining whole IgG was removed using protein A affinity chromatography. Recombinant complement proteins were purchased from Complement Technology, and recombinant protein disulfide isomerase (PDI) was from ProSpec.

Protein expression

Human Trx1 cDNA was obtained from Origene and cloned into pET16b (Novagen) after introduction of NdeI and BamHI restriction sites by PCR. N-terminus His-tagged human Trx1 was then expressed from pET16b in BL21 cells (Invitrogen) after induction with 1 mM isopropyl β -D-1-thiogalactopyranoside (Fermentas). After 3–4 h of expression, bacterial cells were pelleted and resuspended in PBS (Hyclone), cells were lysed using an ultrasonic sonicator (Misonix) and then centrifuged at $10,000 \times g$ for 20 min. His-tagged Trx1 protein was purified from the resultant supernatant using nickel affinity chromatography resin (Qiagen) and dialyzed to TBS (50 mM Tris-HCl and 150 mM NaCl [pH 8]), and aliquots were stored at -80°C . The C32/[³⁵S] and C35S active site mutants were produced from the wild-type plasmid template using the QuikChange site-directed mutagenesis kit (Stratagene), confirmed by sequencing, and expressed and purified in the same way as the wild-type Trx1. Trx80 was produced by site-directed mutagenesis by introducing a stop codon after K80 in the wild-type template. Trx80 was expressed by BL21 cells in inclusion bodies; these were purified by repeated washing of the sonicated lysate pellet with inclusion body wash buffer (50 mM Tris [pH 8], 0.5% Triton X-100, 5 mM EDTA, 100 mM NaCl, and DTT) and then solubilized by dissolving overnight in 6 M urea at 4°C , followed by dialysis first to Tris-EDTA buffer (TBS with 10 mM EDTA) then to PBS before purification of the His-tagged Trx80 by nickel affinity chromatography. Proteins were quantified by using the absorbance at 280 nm and extinction coefficients of $8.05 \text{ mM}^{-1} \text{ cm}^{-1}$ for wild-type and active site mutants of Trx1 and $8.25 \text{ mM}^{-1} \text{ cm}^{-1}$ for Trx80 (4). Purity was assessed by reducing 15% SDS-PAGE. Expected sizes of proteins were 14.1 kDa for His-tagged Trx1 and the CC/SS and C35S mutant forms and 11.5 kDa for His-tagged Trx80. These proteins appeared to run at a higher mass than expected on SDS-PAGE (see Fig. 2A) but were consistent with the apparent size of the non-His-tagged native protein as detected by Western blot analysis of cell

lysates, which also ran slightly higher than expected, compared with the molecular mass ladder (data not shown).

Insulin aggregation assay

To study the activity of Trx1 proteins, an insulin reduction assay was used (24). DTT reduces and therefore activates the Trx1 active site, allowing Trx1 to reduce insulin, which then aggregates. The reduction of insulin by DTT alone is negligible. A total of $100 \mu\text{l}$ $1 \mu\text{M}$ Trx1 protein in PBS was added to $100 \mu\text{l}$ 2 mg/ml bovine insulin (Sigma-Aldrich) in 100 mM KH_2PO_4 and 2 mM EDTA (pH 6.5), with or without 0.5 mM DTT, in wells of a 96-well plate (Nunc). Reduction of insulin and resultant aggregation of the β -chain was followed by measurement of absorbance at 650 nm over time using a microtiter plate reader (Varian). Inhibitory F(ab)₂ was tested by preincubation with Trx1 for 20 min at room temperature before addition of the insulin and DTT.

Analysis of cell surface Trx1

To identify Trx1 at the cell surface, HUVEC were harvested and resuspended in PBS. Cells in PBS/BSA (PBS with 1% BSA) were stained for 30 min with 1:200 diluted rabbit anti-Trx1 serum and washed with PBS/BSA, followed by secondary staining with 1:500 FITC-labeled goat anti-rabbit IgG. Preimmune serum from the same animal was used as a primary Ab control. For chemical labeling, harvested cells were incubated in suspension at 0.5×10^6 cells/ml with 0.5 mg/ml iodoacetyl-PEG₂-biotin (bIAA) (Pierce) or *N*-hydroxy succinimidobiotin (bNHS) (Pierce) for 1 h at 4°C , with rotation. The cells were then washed three times in ice-cold PBS/BSA containing 0.5 M iodoacetamide (Sigma-Aldrich) to quench any remaining free sulfhydryls. The cell pellet was then lysed in lysis buffer (20 mM Tris, 150 mM NaCl, 2 mM EDTA, 0.3% Nonidet P-40, 0.5 mM PMSF, and 0.2 M iodoacetamide [pH 7.5]), and the lysate was incubated for 2 h with Neutravidin beads (Promega) at 4°C . The beads were then washed repeatedly and boiled in SDS-PAGE loading buffer to release proteins, which were blotted for Trx1, or for biotinylated proteins using HRP-conjugated streptavidin (Pierce). Alternatively, biotinylated proteins were isolated from the lysate by use of SoftLink soft release avidin resin (Promega), according to the manufacturer's instructions. Briefly, 500 μl lysate was incubated with avidin resin for 1.5 h at 4°C and washed three times with lysis buffer, and then bound proteins were released using 10% acetic acid before analysis by Western blot using anti-Trx1 Ab. Blots were performed by SDS-PAGE, followed by transfer to polyvinylidene fluoride membrane (Pall), blocked for 1 h with quench buffer (immunowash [50 mM Tris-HCl, 150 mM NaCl, and 0.1% Tween 20 (pH 8)] with 3% fish gelatin [Nordic]) and probed with ATRX04 diluted 1:1000 in quench buffer, or alternatively streptavidin-HRP diluted 1:10,000, for 1 h. For Trx1 blots, membranes were then washed three times in immunowash, and secondary goat anti-rabbit HRP (DakoCytomation) were added at 1:1000 in quench buffer for 1 h. Membranes were then washed again and developed using diaminobenzidine (Sigma-Aldrich).

Hemolytic assays

To study the activity of the classical pathway of complement, sheep RBCs (Swedish National Veterinary Institute) were washed three times in DGVB⁺⁺ buffer (2.5 mM veronal buffer [pH 7.3] containing 70 mM NaCl, 140 mM glucose, 0.1% gelatin, 1 mM MgCl_2 , and 0.15 mM CaCl_2), resuspended to 10^9 cells/ml, and opsonized with an equal volume of amboceptor Ab (Dade Behring) diluted 1:3000 in DGVB⁺⁺, for 20 min at 37°C . The cells were then washed twice in DGVB⁺⁺ buffer before incubation at 8×10^7 cells/ml with 0.3% NHS for 1 h in a V-bottom plate (Nunc) with shaking. Complement-mediated lysis was measured by spinning at 2,000 rpm for 5 min to pellet whole cells and measuring the absorbance of released hemoglobin at 405 nm in the supernatant. To study the alternative activation pathway of complement, rabbit RBCs were washed and resuspended in Mg^{++} EGTA buffer (2.5 mM Veronal buffer [pH 7.3], 70 mM NaCl, 140 mM glucose, 0.1% gelatin, 7 mM MgCl_2 , and 10 mM EGTA) and incubated with 1.25% NHS for 1 h at 37°C in V-bottom plates. Complement-mediated lysis was then measured as described above. To study the ability of Trx proteins or PDI to inhibit the lytic action of complement, thioredoxin proteins were incubated with or without $20 \mu\text{M}$ DTT in DGVB⁺⁺ for 15 min at 37°C before being added to an equal volume of diluted NHS in the appropriate buffer at the above final concentrations. After an additional 15 min at room temperature, RBCs were added and the experiment carried out as described.

Complement deposition assays

Ninety-six-well Maxisorp plates (Nunc) were coated in PBS overnight with $20 \mu\text{g/ml}$ zymosan (Sigma-Aldrich), $5 \mu\text{g/ml}$ aggregated human IgG

(Immuno), or 200 $\mu\text{g/ml}$ mannan (Sigma-Aldrich), which activate the alternative, classical, and lectin pathways, respectively. Plates were then blocked for 1 h with PBS/BSA before incubation with NHS diluted in GVB⁺⁺ buffer (2.5 mM veronal buffer [pH 7.3], 150 mM NaCl, 0.1% gelatin, 1 mM MgCl_2 , and 0.15 mM CaCl_2) for assessment of the classical and lectin pathways and in $\text{Mg}^{++}\text{EGTA}$ for the alternative pathway. Complement activation at 37°C was carried out for 20 min for detection of C3b or 45 min for detection of C5b or C9 for the lectin and classical pathways. For the alternative pathway, incubations were 30 min or 1 h for detection of C3b or C5b and C9, respectively. To assess the inhibitory activity of Trx variants, Trx proteins were preincubated with 20 μM DTT for 15 min at 37°C, then added to an equal volume of NHS, diluted in either GVB⁺⁺ or $\text{Mg}^{++}\text{EGTA}$, and incubated an additional 15 min at room temperature before addition to IgG/zymosan/mannan-coated wells. To assess the activating potential of Trx variants, Trx proteins were coated onto plates at 5 $\mu\text{g/ml}$ in PBS overnight. Wells were then blocked with PBS/BSA for 1 h, and then, NHS were added to the wells diluted to 4% in $\text{Mg}^{++}\text{EGTA}$ buffer for the alternative pathway or to 2% in GVB⁺⁺ for the classical and lectin pathways. Detection of deposited complement proteins was achieved using the specific Abs listed above, added for 1 h in PBS/BSA. After incubation with primary Abs, wells were washed with immunowash, and species-specific HRP-conjugated secondary Abs were added at 1:1000 in PBS/BSA for 1 h. After a final wash with immunowash, the assay was developed using *o*-phenylenediamine dihydrochloride (OPD) tablets (DakoCytomation), according to the manufacturer's instructions, stopped with 0.5 M H_2SO_4 , and the absorbance was read at 490 nm using a Cary microtiter plate reader (Varian).

Binding assays

Purified or recombinant complement proteins were coated overnight in PBS onto 96-well plates at 5 $\mu\text{g/ml}$, blocked with PBS/BSA, and screened by addition of Trx proteins at 5 $\mu\text{g/ml}$ in binding buffer (10 mM HEPES, 150 mM NaCl, 0.5% BSA, 5 mM KCl, 1 mM MgCl_2 , and 2 mM CaCl_2) for 1 h. The plates were then washed three times with immunowash. Binding was detected by addition of polyclonal goat anti-Trx1 (IMCO) diluted 1:1000 in PBS/BSA for 1 h, followed by washing with immunowash, then addition of 1:1000 HRP-conjugated rabbit anti-goat Ab for 1 h, followed by washing and development using OPD tablets. For radioactive assays, Trx proteins were iodinated using chloramine T and [¹²⁵I] and incubated in binding buffer for 2 h in Maxisorp break-apart wells (Nunc) coated overnight with 5 $\mu\text{g/ml}$ complement proteins in PBS and blocked with PBS/BSA. After extensive washing, binding was detected by gamma ray emission using a 1277 Gammamaster gamma counter (Wallac). Competition of binding was prepared by spiking the radiolabeled protein samples with 100 $\mu\text{g/ml}$ unlabeled protein before adding the samples to the plate. For active site capture of Trx1 substrates, the C32[³⁵S] double mutant or the C35S substrate-trapping mutant was used. These proteins were incubated at 5 μM with 5 μM DTT for 15 min at 37°C to reduce cysteine residues and then run through a Zeba desalting spin column (Pierce) to remove DTT. The proteins were then added to 5% NHS in PBS and incubated at 37°C for 1 h. After this, the NHS/Trx1 solution was diluted 6-fold and added to BSA-blocked wells of 96-well plates coated overnight with specific anti-complement Abs to capture possible complement–Trx1 complexes. After 1 h of incubation and washing with immunowash, bound complexes were detected with polyclonal anti-Trx and anti-goat HRP and developed with OPD tablets as described above. The active site-dependent interactions were found by subtracting absorbance values obtained by binding of the Trx CC/SS active site knockout mutant, from values from the Trx C35S substrate-trapping mutant.

Cell surface deposition

For deposition of complement on cell surfaces, HUVEC were plated at 1×10^5 /well in 24-well plates (Sterilin) and left 48 h until confluent. Cells were incubated for 10 min in DGVB⁺⁺ with 4% NHS at 37°C and then complement activated by addition of 100 $\mu\text{g/ml}$ zymosan. After 1 h at 37°C, cells were washed with PBS and detached using TrypLE trypsin replacement (Invitrogen), washed again and then stained for 45 min at 4°C with 1:500 FITC-labeled anti-human C3c (DakoCytomation) in PBS/BSA, or rabbit anti-human sC5b-9neo labeled using Alexa 488 (Invitrogen). Cells were then washed in PBS/BSA and analyzed using a Cyflow space flow cytometer (Partec). The effect of Trx1 on complement deposition was assessed by incubation for 10 min at 37°C with 100 $\mu\text{g/ml}$ anti-Trx1 F(ab)₂, or control F(ab)₂, before the addition of NHS.

Chemotaxis assays

Refludan plasma was diluted to 3% in $\text{Mg}^{++}\text{EGTA}$ buffer and incubated with 0.5 $\mu\text{g/ml}$ zymosan (Sigma-Aldrich) or 5 μM Trx80 for 1 h at 37°C

with gentle rocking, in the presence of 1.5 mM Plummer's inhibitor (Pierce) and 50 mM 6-amino hexanoic acid (Carl Roth) to prevent C5a degradation. To test the effect of Trx1, 5 μM Trx1 was activated by incubation with 20 μM DTT in $\text{Mg}^{++}\text{EGTA}$ buffer for 15 min at 37°C and then added to an equal volume of 6% Refludan plasma before the addition of zymosan. After activation, the plasma was spun at $18,000 \times g$ for 1 h at 4°C to pellet protein complexes and particles and then immediately stored at –80°C in aliquots until tested. Activated plasma samples were loaded into the lower wells of a chemotaxis chamber (Neuro Probe), and 50 μl human neutrophils was loaded into the upper wells at a density of 3×10^6 /ml in PBS. Wells were separated by polycarbonate membranes with a pore size of 3 μm (Neuro Probe). To assess the C5a dependence of neutrophil chemotaxis toward the lower wells, all samples were run in parallel using neutrophils preincubated for 15 min at room temperature with 100 nM C5a receptor (C5aR)/C5L2 antagonist (C5aRA) (25). After 30 min of incubation at 37°C, the chamber was disassembled, and the membrane was washed, fixed, and stained using a Pappenheim stain (May–Grunwald stain followed by Giemsa stain; Merck), images were taken using a $\times 100$ oil immersion Eclipse 50i microscope (Nikon), and the number of cells per field was counted. Three images were taken per well, and all wells were performed in triplicate.

C3a production in serum

Trx1 or Trx80 were incubated in 20% NHS in GVB⁺⁺ buffer for 15 min at 37°C. Aliquots of sample (10 μl) were then immediately boiled in nonreducing loading buffer, separated on a 15% SDS-PAGE, transferred to polyvinylidene difluoride membrane, and C3a detected using a specific Ab. Strength of bands was assessed by densitometry using ImageGauge software. The background value of C3a produced in NHS alone (by spontaneous alternative pathway tickover) was subtracted, and results were expressed relative to positive control of NHS incubated with 250 $\mu\text{g/ml}$ zymosan.

In vivo peritonitis model

OVA (20 mg/kg body weight; Sigma-Aldrich) was injected i.v., followed by an i.p. injection of IgG rich in Ab against OVA (800 $\mu\text{g}/\text{mouse}$; ICN) as described previously (26). One group of the C57BL/6J mice was pretreated with 200 μg Trx1 i.v. 30 min prior to the onset of the immune complex-peritonitis. Mice were then sacrificed 6 h after injury, and the peritoneal cavity was lavaged with 5 ml PBS and 0.1% BSA. Peritoneal cells were stained with anti-Ly-6G mAbs and analyzed by flow cytometry (LSRII; BD). Ly-6G^{hi} neutrophil numbers were enumerated using BD True count beads. These studies were reviewed and approved by the Ministerium für Landwirtschaft, Umwelt und ländliche Räume (Kiel, Germany). The amounts of Trx1 given per mouse were based on expected pharmacokinetic behavior of a protein of this size.

Statistical analysis

Statistical analysis was carried out using Graphpad Prism 5.0. Statistical significance was assessed by one-way ANOVA, or two-way ANOVA for experiments with multiple variables, with Bonferroni posttest. For comparison of only two groups, *t* test was used.

Results

Trx1 is present in a reduced form at the endothelial cell surface and limits MAC deposition

Trx1 is expressed at the cell surface in various cell types, including human endothelial cells and leukemic cells (27, 28). To confirm this, we stained HUVEC with rabbit anti-Trx1 serum, using pre-vaccination serum from the same animal as a negative control (Fig. 1A). A total of 91.5% of cells were stained positive compared with negative control. Trx reductase, which catalyzes the activation of Trx1 in the intracellular environment, has not been identified as a cell surface protein, so it is uncertain whether Trx1 at the cell surface would be in an oxidized, inactive state or a reduced and active state. To address this, HUVEC surface-reduced thiols were labeled with non-cell membrane-permeable bIAA, using bNHS as a positive control to label all cell surface proteins via primary amines. Labeled HUVEC lysates analyzed by Western blotting for Trx1 and biotin showed equally sized bands (Fig. 1B), and Trx1 was also immunoprecipitated using neutravidin beads

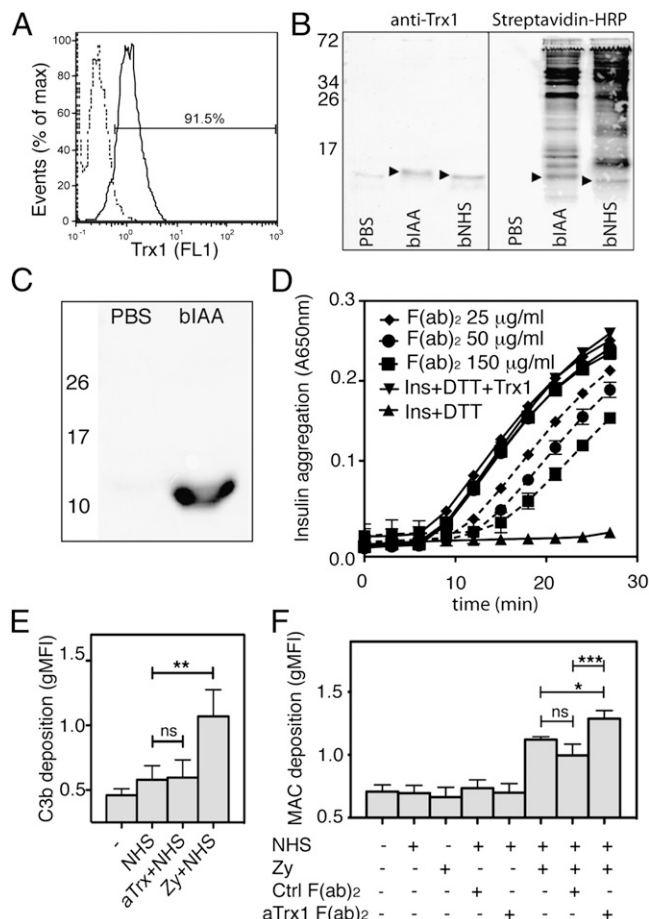


FIGURE 1. Trx1 is present on the cell surface of HUVEC in a reduced form and limits MAC deposition. **(A)** Detection of Trx1 on HUVEC by flow cytometry using rabbit anti-Trx1 serum (solid line) and preimmune serum from the same animal as a negative control (broken line). A number denotes percentage of cells staining positive for Trx1, gated above the 95th percentile of the negative control. **(B)** Western blots of HUVEC lysates after incubation of cells with PBS or non-membrane-permeable bIAA or bNHS to label surface proteins. Lysates were blotted for Trx1 (left panel) or biotin (right panel). **(C)** Western blot for Trx1 after use of neutravidin beads to precipitate biotinylated proteins from HUVEC lysates after cells were incubated with either PBS or bIAA. Each experiment was performed independently three times with similar results. **(D)** Trx1 activity can be assessed using an insulin assay, where in the presence of DTT, Trx1 causes reduction of insulin and subsequent aggregation of the liberated insulin β -chain, measurable by absorbance at 650 nm. The addition of Trx-specific F(ab)₂ (broken lines), but not nonspecific F(ab)₂ (solid lines), inhibits Trx1 activity in a concentration-dependent manner. **(E)** HUVEC were incubated with F(ab)₂ and NHS for 1 h at 37°C and C3b deposition was assessed by flow cytometry. **(F)** Preincubation of HUVEC with blocking Trx-specific F(ab)₂ caused an increase in zymosan-mediated MAC deposition. **(A)–(D)** are each representative of three independently performed experiments. Data in **(E)** and **(F)** are shown as means of three independent experiments performed in duplicates with bars indicating SD. Statistical significance of differences was calculated using one-way ANOVA with Bonferroni post-test with * $p < 0.05$, ** $p < 0.01$, *** $p < 0.005$. **(B)** and **(C)** Numbers indicate molecular mass markers in kilodaltons.

from lysates from bIAA-labeled HUVEC, but not from unlabeled cells (Fig. 1C). These results show that Trx1 is found at the cell surface of human endothelial cells in a reduced and therefore enzymatically active form.

To assess whether cell surface Trx1 affects complement deposition, a blocking anti-Trx1 F(ab)₂ fragment was produced. Protein A-purified whole IgG from Trx1-vaccinated rabbit serum was

digested using pepsin, and the Trx-specific fraction was separated using an immobilized Trx1 column. The Trx-specific, but not the nonspecific fraction was able to partially inhibit the enzymatic activity of Trx1 (Fig. 1D). The Trx-specific F(ab)₂ fragment was then used to block cell surface Trx1 to assess the effect on complement deposition. As evidence for the absence of whole IgG, which could trigger the classical pathway, no C3 deposition could be detected after 1-h incubation of HUVEC with F(ab)₂ and NHS (Fig. 1E). However, the preincubation of HUVEC with blocking F(ab)₂, but not nonspecific F(ab)₂, caused an increase in zymosan-mediated MAC deposition (Fig. 1F). This suggests a role for cell surface Trx1 as an inhibitor of complement deposition.

Trx1 inhibits complement in an active site-dependent manner

To study its function, human Trx1 was expressed in BL21 cells with an N-terminal His tag and purified by nickel ion chromatography. In addition to the wild type, a mutant form was expressed with the active site cysteines at positions 32 and 35 replaced with serine residues (Trx CC/SS), as well as the truncated form, Trx80 (Fig. 2A). These proteins ran slightly higher than their expected molecular masses of 14.1 and 11.5 kDa, but this was consistent with

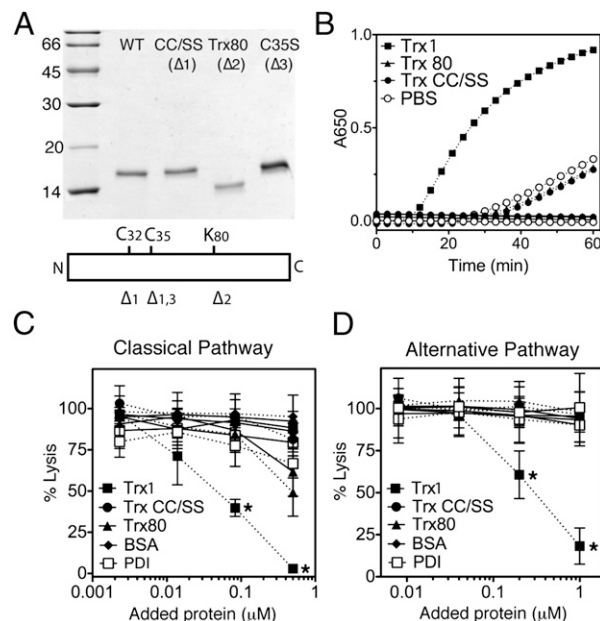


FIGURE 2. Trx1 inhibits complement-mediated hemolysis in an active site-dependent manner. **(A)** Reducing 15% SDS-PAGE of purified His-tagged Trx1 (wild-type [WT], active site mutants, and Trx80), followed by silver staining. Lower panel shows schematic of Trx1 protein with mutation sites. Δ_1 : CC/SS variant, C32 and C35 mutated to S; Δ_2 : Trx80 variant, stop codon inserted after K80; and Δ_3 : C35S variant, C35 only mutated to S. **(B)** Functional testing of purified Trx proteins by an insulin reduction assay. Trx proteins and insulin were mixed in the presence (broken lines) or absence (solid lines) of DTT and aggregation of the reduced insulin β -chain followed by absorbance at 650 nm. **(C)** Sheep RBCs opsonized with Ab were incubated with NHS in DGVB⁺⁺ buffer, and lysis was measured by the absorbance of released hemoglobin in the supernatant at 490 nm. Trx proteins were added in the presence (broken lines) or absence (solid lines) of 10 μ M DTT. **(D)** The effect of Trx proteins on lysis triggered via the alternative activation pathway of complement was studied as in **(C)**, but using rabbit RBCs in Mg⁺⁺EGTA buffer, which allows the activation of the alternative pathway of complement only. **(A)** and **(B)** are representative examples of three independently performed experiments. Results shown in **(C)** and **(D)** are the averages of three independent experiments performed in duplicate with error bars denoting SD. Statistical analysis was performed by two-way ANOVA. * $p < 0.005$ as compared with BSA.

endogenous Trx1, which also ran at a higher than expected mass as detected by Western blots of cell lysates (data not shown). The enzymatic function of purified Trx variants was demonstrated in an insulin reduction assay, causing aggregation and an increase in absorbance at 650 nm (Fig. 2B). The dependency of Trx1 activity on the presence of DTT reflects the need for reduced cysteine residues in the Trx1 active site. As expected, Trx80 and the Trx CC/SS active site mutant have no reductase activity even in the presence of DTT (Fig. 2B).

Uninhibited activation of complement by any of the three canonical pathways (classical, lectin, and alternative) results in the formation of MAC, which inserts into and breaches cell membranes. The ability of Trx1 to inhibit MAC formation was tested using hemolytic assays. The lysis of sheep RBCs via the classical complement activation pathway and lysis of rabbit RBCs via the alternative complement activation pathway were both inhibited by the addition of Trx1 in the presence 10 μ M DTT (Fig. 2C, 2D), with inhibition of the classical pathway starting at 10 nM Trx1 and reaching complete inhibition by 500 nM ($p < 0.005$). Classical activation pathway lysis was unaffected by PDI, a disulfide-reducing enzyme containing two CXXC Trx-family active sites, which has also been identified at cell surfaces (29), implying specificity to the Trx-complement interaction. Inhibition of the alternative pathway by Trx1 was as statistically significant ($p < 0.005$) but required higher concentrations. In the absence of DTT, there was no inhibition of either pathway, indicating that the mechanism is active site dependent. This was supported by the use of Trx CC/SS and Trx80, which having no reductase activity, were unable to inhibit lysis regardless of DTT presence.

Trx1 inhibits deposition of C5b-9, but not C3b

To determine the stage of the complement activation cascade at which Trx1-mediated inhibition occurs, deposition assays were performed. Wells of 96-well plates were coated with aggregated IgG, mannan, or zymosan, which activate the classical, lectin, and alternative pathways, respectively, and the effect of Trx1 on deposition of individual complements components assessed (Fig. 3). C1q, MBL, ficolin, and C4b deposition, early results of activation of the classical or lectin pathways, were not affected (data not shown). C3b deposition, an early step of all three pathways, was also unaffected, but deposition of C5b and C9 was subject to a concentration-dependent inhibition by Trx1 with an effect on C5b deposition from 10 nM Trx1 in the classical and lectin pathways and an inhibition of C9 deposition starting at 10 nM Trx1 in all three pathways. Inhibition by wild-type Trx1 was active site dependent, because deposition was unaffected by the presence of Trx CC/SS or Trx80 regardless of the presence of DTT.

Trx80 binds to initiators and inhibitors of complement, whereas full-length Trx1 interacts only with inhibitors

To identify which complement factors Trx1 interacts with, Trx proteins were screened for binding to complement components. Unexpectedly, Trx80 rather than Trx1 interacted most strongly with complement proteins, specifically the C1q complex, properdin, and C4BP, but not factor H or other complement components (Fig. 4A). These results were confirmed by the concentration-dependent binding of 125 I-labeled Trx80, but not labeled wild-type or CC/SS Trx1 (Fig. 4B). Curiously, 125 I-labeled Trx80 was detected bound to factor H, whereas Ab detection of unlabeled Trx80 to factor H could not be shown.

In comparison with Trx80, the full-length Trx1 did not interact with complement components in binding assays. The complement inhibitory activity of Trx1 is active site dependent, and therefore,

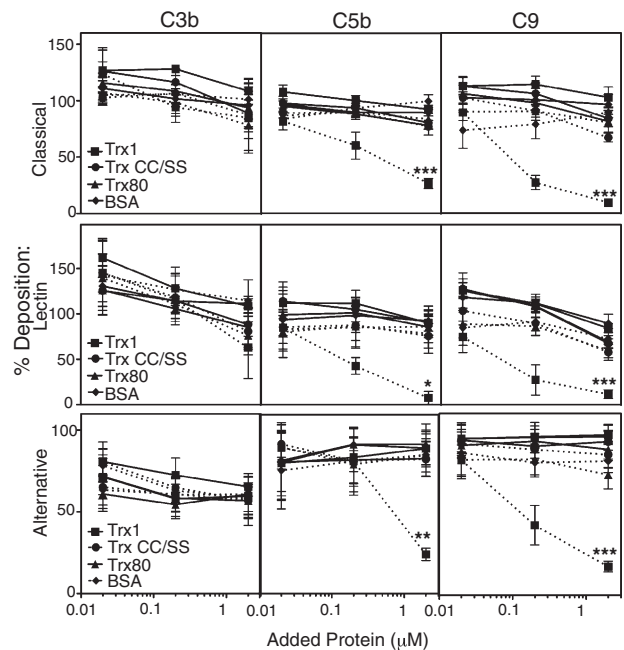


FIGURE 3. Trx1 inhibits activation of complement at the level of the C5 convertase. Plates were coated with aggregated human IgG, mannan, or zymosan to trigger the classical, lectin, or alternative pathways, respectively. Plates were then incubated with NHS with varying amounts of Trx proteins, in GVB⁺⁺ buffer for the classical and lectin pathways, and Mg⁺⁺ EGTA buffer for the alternative pathway, either with DTT (broken lines) or without (solid lines). After incubation and washing, deposition of complement products was assessed by detection using specific Abs. A significant Trx1-dependent reduction in deposition of the MAC components C5b and C9 was detected in all three pathways. Each condition was performed in duplicate. Results are the average of three independent experiments. Error bars represent SD; statistical analysis was performed using two-way ANOVA: * $p < 0.05$, ** $p < 0.01$, *** $p < 0.005$.

the interaction of Trx1 with its substrate may be transient and not detectable in assays dependent on stable binding. We therefore produced a second active-site mutant, Trx C35S, which forms a stable mixed disulfide with its substrate, the cysteine residue at position 35 being required for completion of the enzymatic disulfide reductase reaction and release of the substrate. This substrate-trapping mutant was able to capture factor H from serum, confirming the previously reported interaction (13) but also demonstrated an equal interaction with C4BP (Fig. 4C).

Trx80 triggers limited complement deposition

C1q and properdin (30), which bind Trx80, are able to cause activation of the classical and alternative pathways respectively, and we therefore hypothesized that Trx80 can trigger complement deposition by the classical and alternative pathways. Activation of these pathways was tested by coating Trx80 onto plates and incubated with NHS in GVB⁺⁺ or Mg⁺⁺EGTA, respectively. Binding of MBL or ficolins 2 or 3 (all initiators of the lectin pathway of complement activation) was not detected, but Trx80 did show binding by C1q from human serum (Fig. 5A). Trx80, but not Trx1, was able to cause significant deposition of C4b and C3b ($p < 0.001$ for Trx80, compared with $p > 0.05$ for Trx1, for both C4b and C3b), with deposition being comparable to a positive control of aggregated IgG (Fig. 5B). However, late-stage complement activation was far weaker, with little detected deposition of C5b or C9. The same was true when deposition was carried out in Mg⁺⁺EGTA buffer, which prevents activation of the classical or lectin pathways, while allowing alternative pathway activation. Signifi-

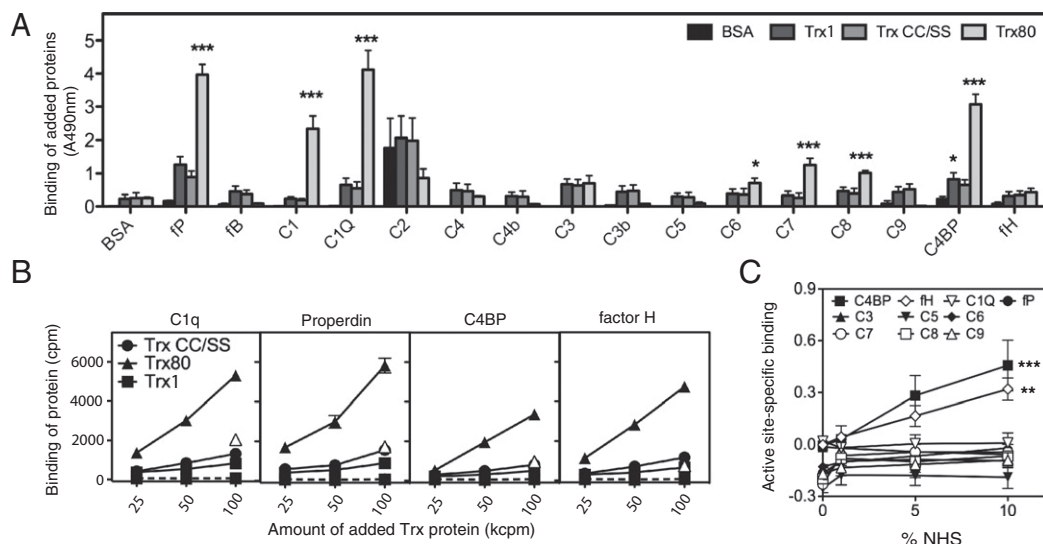


FIGURE 4. Trx80 interacts with initiators and inhibitors of complement. **(A)** Complement proteins were coated onto 96-well plates at 5 μ g/ml and probed with Trx proteins. Binding was detected using polyclonal anti-Trx, which detects both Trx1 and Trx80, compared with BSA. **(B)** 125 I-labeled Trx proteins were coated to plates coated with complement proteins (solid lines) or BSA (broken lines) and washed, and binding was detected by gamma ray emission. Specificity of binding of [125 I]Trx80 was determined by the addition of excess, unlabeled Trx80 as competition during the binding incubation (open triangles). **(C)** The active-site substrates of Trx1 were investigated using the C35S substrate-trapping mutant of Trx1. Only C4BP and factor H were captured from serum by the C35S mutant in comparison with binding by the CC/SS active site knockout mutant. The difference in binding between C35S and CC/SS was used to determine the active-site specific interaction. ** $p < 0.01$ and *** $p < 0.005$ by two-way ANOVA. All results in this figure show the averages of at least three independent experiments carried out in duplicates; error bars represent SD. fB, Factor B; fH, factor H; fP, properdin.

cant levels of C3b, but little C9, was deposited from serum in Mg^{++} EGTA buffer in wells coated with Trx80 (Fig. 5C).

In previous binding assays, factor H binding to Trx80 could be detected using 125 I-Trx80, but not when using anti-Trx80 Abs to

detect Trx80 bound to immobilized factor H. We therefore hypothesized that factor H, a 150 kDa protein, does interact with Trx80 but in such a way as to block Ab binding epitopes on Trx80, preventing Ab detection of Trx80, whereas gamma emission from

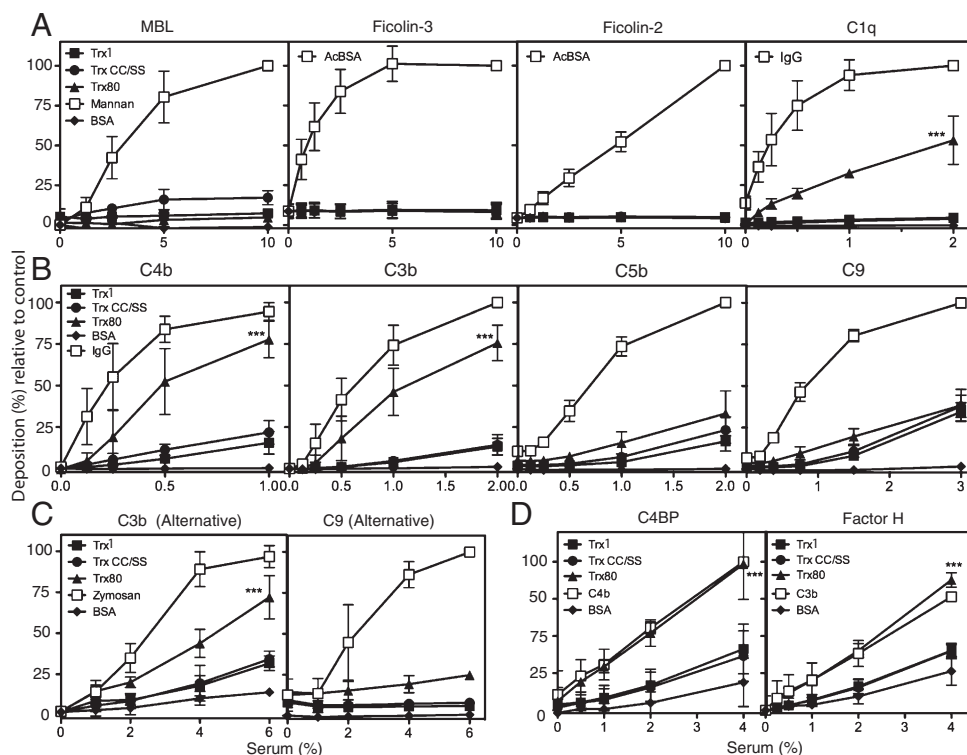


FIGURE 5. Trx80 triggers limited activation of complement via the classical and alternative pathways. Plates were coated with Trx proteins or BSA, incubated with NHS, and deposited complement proteins detected with specific Abs. **(A)** Trx80 is bound by C1q from NHS, but not by activators of the lectin pathway. **(B)** Trx80 causes significant deposition of C4b and C3b as a result of complement activation, but not of C5b or C9, components of the MAC. **(C)** Similar deposition of C3b, but not C9 was seen in the alternative pathway, carried out in Mg^{++} EGTA buffer. **(D)** C4BP and factor H also both bind Trx80 from serum. Results shown are averages of at least three independent assays with each condition performed in duplicate. Error bars represent SD. *** $p < 0.005$ by two-way ANOVA, compared with binding to or deposition onto coated BSA.

125 I-labeled Trx80 is still detectable. In support of this hypothesis, factor H binding from heat inactivated NHS (hiNHS) to immobilized Trx80 could be detected by anti-factor H Ab (Fig. 5D). The binding of C4BP to Trx80 from hiNHS was also confirmed (Fig. 5D). The detected binding of C4BP and factor H to Trx80 was equal to their binding of known ligands C4b and C3b.

Trx1 and Trx80 have opposing effects on anaphylatoxin production

It has previously been described that Trx1 and Trx80 have differing functions, with Trx80 lacking the enzymatic activity of Trx1, and causing release of proinflammatory cytokines from (5, 31), and enhancing bacterial killing by (32), monocytes. With Trx1 and Trx80 also having opposing effects on complement, we tested their effects on C5a production. We performed chemotaxis assays to measure the C5a-dependent migration of human neutrophils. Trx1 was able to inhibit C5a production in Mg^{++} EGTA-diluted human plasma activated by zymosan, an activator of the alternative pathway, as measured by a decrease in neutrophil chemotaxis (Fig. 6A). In contrast, Trx80 was able to stimulate C5a production in plasma, resulting in increased chemotaxis (Fig. 6B). Addition of C5aRA reduced all chemotaxis to background levels, indicating that the observed chemotaxis was mediated specifically by C5a–C5aR interactions. In addition, incubation of Trx80, but not Trx1,

with NHS induced production of C3a, as detectable by Western blot, above the background level of C3a produced by alternative pathway tickover (Fig. 6C). During this short incubation time, levels of C3a saturated at only 50 nM Trx80. To titrate the activation of complement by Trx80 with more sensitivity, Trx80 was coated onto plates at serial dilutions, with aggregated IgG and Trx1 as positive and negative controls. Plates were incubated with 2% NHS for 20 min before detection of deposited C3b. Trx80 caused significant levels of deposition, as compared with wells of Trx80 incubated with hiNHS (Fig. 6D). Deposition of C3b by Trx80 was detectable at lower concentrations than IgG, with deposition being significantly higher than all controls at a lowest titration of 62 ng/ml, by one-way ANOVA (Fig. 6E). This is within the physiological range of Trx80 as measured in plasma of healthy controls (4).

Trx1 inhibits complement-mediated neutrophil chemotaxis in vivo

To validate the inhibitory effect of Trx1 in vivo, reverse passive Arthus (RPA) reactions were carried out by i.v. injection of OVA followed by i.p. injection of anti-OVA Ab. The pretreatment of animals with Trx1 caused a significant inhibition of neutrophil chemotaxis to the site of immune complex formation (Fig. 7).

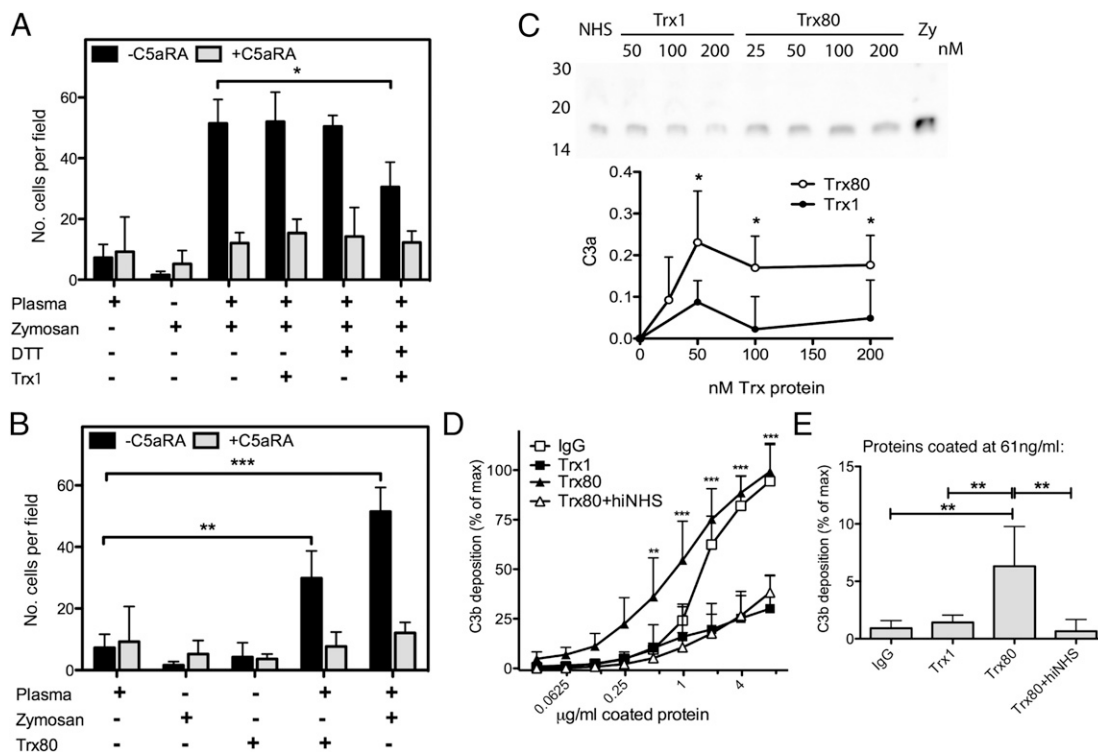


FIGURE 6. Trx1 and Trx80 have opposing effects on anaphylatoxin production from plasma. C5a presence was assayed by chemotaxis of neutrophils through a 3- μ m pore size membrane, which was fixed and stained, and numbers of cells per field of a $\times 100$ light microscope were counted. To assess the C5a receptor dependency of chemotaxis, cells run with samples in parallel were preincubated with 100 nM C5aRA. **(A)** Plasma diluted to 3% in Mg^{++} EGTA was incubated for 1 h at 37°C in the absence or presence of zymosan, DTT, and Trx1. Activated plasma was then assayed for C5a presence in a chemotaxis chamber. Trx1 significantly reduced neutrophil chemotaxis in the presence of DTT. * $p < 0.05$. **(B)** Plasma was incubated 1 h at 37°C with either zymosan or 5 μ M Trx80. Both Trx80 and zymosan induced significant C5aR-dependent migration. Results represent mean values from three independent experiments, with three fields counted per well, and all wells were in triplicates. Error bars show SD. ** $p < 0.01$ and *** $p < 0.005$ by one-way ANOVA with Bonferroni posttest compared with plasma + zymosan in (A) and plasma alone in (B). **(C)** C3a production by Trx1 or Trx80 incubated in NHS was detected by Western blot. *Upper panel*, Representative example of gel results. Size markers are shown in kilodaltons. *Lower panel*, C3a was quantified by densitometry of gel bands, and values above background (NHS incubated alone) were normalized against C3a produced after incubation with zymosan. Results show mean and SD from five independent repeats. * $p < 0.05$ by two-way ANOVA. **(D)** Trx proteins were coated onto a plate at the given concentrations, blocked, and incubated with 2% NHS for 20 min before deposited C3b was detected as described previously. ** $p < 0.01$ and *** $p < 0.005$ by two-way ANOVA, compared with Trx80 in hiNHS. **(E)** C3b deposition by Trx80 and controls coated at 62 ng/ml. ** $p < 0.01$ by one-way ANOVA. (C and D) Results represent means and SD from four independent experiments. NHS, NHS incubated alone; Zy, NHS incubated with zymosan.

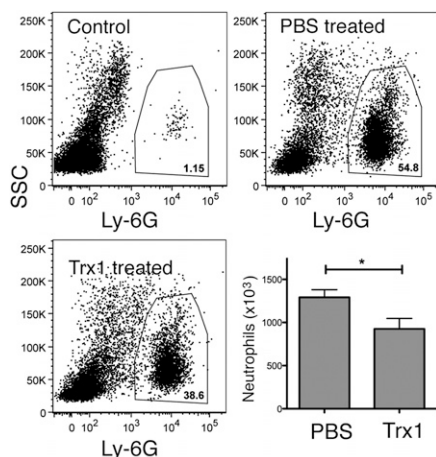


FIGURE 7. Trx1 inhibits immune complex-mediated neutrophil recruitment in vivo. The RPA was carried out in BABL/c mice. Treatment groups were injected i.v. with 200 μ g/ml Trx1 before initiation of the RPA. After 6 h, neutrophil chemotaxis to the site of immune complex formation was assessed by flow cytometry. Representative FACS plots are shown. The data are representative of two independent experiments; four mice per group. * $p < 0.05$ according to t test.

Discussion

A previous study has indicated that Trx1 is able to inhibit complement activation in mice after laser burn injury, leading to a reduction in choroidal neovascularization (13). Complement has indeed been implicated in the activation and stimulation of endothelial cells (33), with the subsequent release of proangiogenic and prothrombotic factors (34). In this study, we have further investigated the mechanism of complement inhibition by Trx1 and demonstrated the presence of reduced Trx1 at the endothelial cell surface, suggesting a role in limiting cell surface complement deposition. C5a and MAC can both activate endothelium (33, 35, 36), leading to upregulation of adhesion molecules. In addition, production of C5a attracts neutrophils, and combined with adhesion molecule upregulation, this can contribute to endothelial damage. Trx1 could therefore limit endothelial activation, cell damage, and resultant thrombosis.

Trx1 has recently been shown to interact with the innate immune system by reducing and therefore activating human β -defensin 1 (37), promoting antibacterial activity. Our study now shows that it also interacts with the complement system, limiting the deposition of terminal activation products. These two opposing activities may at first seem counterproductive. However, we found that Trx1 inhibits MAC, but not C3b deposition, a major and important step in complement activation. The opsonization of bacteria by C3b greatly enhances phagocytosis, whereas MAC only plays a role in killing a limited number of bacterial species, with MAC-component-deficient individuals suffering only from an increased susceptibility to neisserial infections (38). The role of cell surface Trx1 may rather be more important in the localized inhibition and protection of self-surfaces, because soluble Trx1 in serum rapidly becomes oxidized and therefore enzymatically inactive (39). In addition, the roles of Trx1 may differ at different anatomical locations, with β -defensin 1 being present at epithelial sites, whereas complement is found at highest concentrations in serum at endothelial surfaces. The mechanism by which Trx1 inhibits complement appears to be related to its effect on C5 (and perhaps also C3) convertases. We conclude this based on the fact that we observe a clear inhibitory effect of Trx1 in hemolytic assays of both the classical and the alternative pathways. Deposition assays for all three complement pathways showed that Trx1 attenuates

deposition of C5b and C9. Because no clear interactions with single purified complement components and Trx1 were detected, we find it most plausible that Trx1 binds to and inhibits assembled convertases.

Trx1 is found at elevated levels in serum of individuals with a wide range of diseases, reaching highest recorded levels in patients suffering fatal sepsis (3). Complement activation products, particularly C5a, are also implicated in the pathogenic consequences of sepsis (40). It is currently hypothesized that Trx1 is released into serum from the cell surface once oxidized (41), after conversion to a form in which it no longer has functional active site activity. This could occur during oxidative stress or because of the enzymatic activity of the enzyme itself, which leaves the substrate reduced and Trx1 oxidized. It could therefore be hypothesized that an exhaustion of functional cell surface Trx1 contributes to the pathogenesis of sepsis because of a loss of control of complement activation. Indeed, it has been shown that transgenic overexpression of Trx1 leads to greater survival in sepsis, whereas injection of neutralizing anti-Trx1 Abs increases mortality in an animal model (3), demonstrating a protective effect of functional Trx1. Although demonstrated as being efficacious in animal models of disease (3, 7, 13, 41), the precise mechanism of function has not been definitively proven, and we suggest that further investigation into the effect of Trx1 on complement activation in sepsis, and other diseases, should be carried out.

We also demonstrated that Trx1 reduced neutrophil influx in vivo in a peritoneal reverse RPA model. Inflammation caused by RPA depends on FcR and complement-mediated mechanisms (42–44), with early involvement of mast cells (45, 46) and later contribution of macrophages (45). Several studies in which the C5aR has been pharmacologically targeted or genetically deleted provide compelling evidence for a critical role of C5a in initiating the inflammatory cascade in immune complex peritonitis (26, 47). However, genetic deletion of either the C5aR (47) or C5 (48) resulted in variable and sometimes incomplete (47) protection from neutrophilic inflammation. Also, depending on the dose and the site of administration, C5aR blockade leads to variable inhibition of neutrophil recruitment into the peritoneal cavity (26, 45). In line with such findings, administration of Trx1 significantly but incompletely inhibited peritoneal neutrophil influx following immune complex formation. Taken together with our findings that Trx1 inhibits the classical pathway of complement and the cleavage of C5, these data suggest that Trx1 may prove useful as a therapeutic agent for complement-mediated pathologies, although it was less effective than reported effects of C5aRA (26, 45). This reduced efficiency of Trx1 complement inhibition activity could be due to a lower specificity of action compared with reagents such as C5aRA. Further optimization of Trx1 dosage could lead to more effective therapy.

In contrast to the complement-inhibitory activities of Trx1, the truncated form, Trx80, was able to bind to complement initiators C1q and properdin, leading to activation of the complement cascade and production of the anaphylatoxin C5a. The ability of Trx80 to cause C5a production, but very low levels of C5b deposition, insinuates C5 cleavage, but limited binding of C5b to C6 and C7, which then becomes deposited on surfaces. A lack of formation of C5b67 would therefore prevent full MAC formation, which occurs after binding of C8 and polyC9. A possible mechanism for this could be the binding of Trx80 to individual MAC components, which was detected in initial binding screens (Fig. 4A). The binding of both factor H and C4BP would also limit the activation caused by Trx80 at the level of convertase formation, which should be then most apparent during measurement of deposition of C5b/MAC. This is also in agreement with observations that many

endogenous molecules that act as danger signals and activate complement via interaction with C1q, also bind C4BP and factor H to limit the inflammatory final steps of the complement cascade (49–51). The production of C3a by Trx80 was significantly higher than by Trx1 at nanomolar amounts, and deposition of C3b could be triggered by Trx80 coated onto plates at physiological nanomolar concentrations. Although levels of Trx80 have been measured in healthy individuals at up to 174 ng/ml (4), this may be higher in disease or in local environments. For example, Trx80 secretion has been identified in synoviocytes from rheumatoid arthritis patients, but not osteoarthritic controls, and therefore, Trx80 could be expected to be elevated in rheumatoid arthritis synovial fluid (52).

It has already been described that Trx1 and Trx80 have contrasting roles in respect to their disulfide reductase activities and their respective anti- or proinflammatory properties (41, 53). The mechanism of formation of Trx80 found in serum is not currently understood. Although there is evidence suggesting that it is formed from the full-length form after cleavage at the surface of activated macrophages (54), we could not reproduce these results. However, because of the ability of Trx80 to generate levels of C5a, the mechanism of conversion of Trx1 to Trx80 could act as a molecular switch from an inhibitory to an activatory molecule, and therefore, this mechanism must be fully understood before consideration of Trx1 for use as a therapeutic. Particularly in inflammatory conditions where expression of candidate proteases may be upregulated, application of Trx1 for anti-inflammatory purposes could lead instead to in vivo conversion of the protein to Trx80, leading to undesired complement activation and increased inflammation.

Acknowledgments

We are grateful to Prof. Arne Holmgren (Karolinska Institute) for valuable advice, Prof. Peter Garred (University of Copenhagen) for contribution of reagents, and Tom Groeneveld and Gia Ky Vuong for technical assistance.

Disclosures

The authors have no financial conflicts of interest.

References

- Jones, D. P. 2008. Radical-free biology of oxidative stress. *Am. J. Physiol. Cell Physiol.* 295: C849–C868.
- Rubartelli, A., A. Bajetto, G. Allavena, E. Wollman, and R. Sitia. 1992. Secretion of thioredoxin by normal and neoplastic cells through a leaderless secretory pathway. *J. Biol. Chem.* 267: 24161–24164.
- Hofer, S., C. Rosenhagen, H. Nakamura, J. Yodoi, C. Bopp, J. B. Zimmermann, M. Goebel, P. Schemmer, K. Hoffmann, K. Schulze-Osthoff, et al. 2009. Thioredoxin in human and experimental sepsis. *Crit. Care Med.* 37: 2155–2159.
- Pekkari, K., R. Gurunath, E. S. Arner, and A. Holmgren. 2000. Truncated thioredoxin is a mitogenic cytokine for resting human peripheral blood mononuclear cells and is present in human plasma. *J. Biol. Chem.* 275: 37474–37480.
- Pekkari, K., J. Avila-Cariño, A. Bengtsson, R. Gurunath, A. Schevinius, and A. Holmgren. 2001. Truncated thioredoxin (Trx80) induces production of interleukin-12 and enhances CD14 expression in human monocytes. *Blood* 97: 3184–3190.
- Nakamura, H., L. A. Herzenberg, J. Bai, S. Araya, N. Kondo, Y. Nishinaka, L. A. Herzenberg, and J. Yodoi. 2001. Circulating thioredoxin suppresses lipopolysaccharide-induced neutrophil chemotaxis. *Proc. Natl. Acad. Sci. USA* 98: 15143–15148.
- Zhang, J., F. Chen, T. Nakamura, T. Fujinaga, A. Aoyama, H. Hamakawa, H. Sakai, Y. Hoshino, J. Yodoi, H. Wada, et al. 2009. Protective effect of thioredoxin perfusion but not inhalation in warm ischemic-reperfused rat lungs. *Redox Rep.* 14: 75–81.
- Shibuki, H., N. Katai, S. Kuroiwa, T. Kurokawa, J. Yodoi, and N. Yoshimura. 1998. Protective effect of adult T-cell leukemia-derived factor on retinal ischemia-reperfusion injury in the rat. *Invest. Ophthalmol. Vis. Sci.* 39: 1470–1477.
- Fukuse, T., T. Hirata, H. Yokomise, S. Hasegawa, K. Inui, A. Mitsui, T. Hirakawa, S. Hitomi, J. Yodoi, and H. Wada. 1995. Attenuation of ischaemia reperfusion injury by human thioredoxin. *Thorax* 50: 387–391.
- Tao, L., E. Gao, N. S. Bryan, Y. Qu, H. R. Liu, A. Hu, T. A. Christopher, B. L. Lopez, J. Yodoi, W. J. Koch, et al. 2004. Cardioprotective effects of thioredoxin in myocardial ischemia and reperfusion: role of S-nitrosation [corrected]. [corrected] *Proc. Natl. Acad. Sci. USA* 101: 11471–11476.
- Arumugam, T. V., I. A. Shiels, T. M. Woodruff, D. N. Granger, and S. M. Taylor. 2004. The role of the complement system in ischemia-reperfusion injury. *Shock* 21: 401–409.
- Czermak, B. J., V. Sarma, C. L. Pierson, R. L. Warner, M. Huber-Lang, N. M. Bless, H. Schmal, H. P. Friedl, and P. A. Ward. 1999. Protective effects of C5a blockade in sepsis. *Nat. Med.* 5: 788–792.
- Inomata, Y., H. Tanihara, M. Tanito, H. Okuyama, Y. Hoshino, T. Kinumi, T. Kawaji, N. Kondo, J. Yodoi, and H. Nakamura. 2008. Suppression of choroidal neovascularization by thioredoxin-1 via interaction with complement factor H. *Invest. Ophthalmol. Vis. Sci.* 49: 5118–5125.
- Haines, J. L., M. A. Hauser, S. Schmidt, W. K. Scott, L. M. Olson, P. Gallins, K. L. Spencer, S. Y. Kwan, M. Noureddine, J. R. Gilbert, et al. 2005. Complement factor H variant increases the risk of age-related macular degeneration. *Science* 308: 419–421.
- Ricklin, D., G. Hajishengallis, K. Yang, and J. D. Lambris. 2010. Complement: a key system for immune surveillance and homeostasis. *Nat. Immunol.* 11: 785–797.
- Köhl, J. 2006. The role of complement in danger sensing and transmission. *Immunol. Res.* 34: 157–176.
- Ricklin, D., and J. D. Lambris. 2007. Complement-targeted therapeutics. *Nat. Biotechnol.* 25: 1265–1275.
- Bora, P. S., J. H. Sohn, J. M. Cruz, P. Jha, H. Nishihori, Y. Wang, S. Kaliappan, H. J. Kaplan, and N. S. Bora. 2005. Role of complement and complement membrane attack complex in laser-induced choroidal neovascularization. *J. Immunol.* 174: 491–497.
- Amara, U., M. A. Flierl, D. Rittirsch, A. Klos, H. Chen, B. Acker, U. B. Brückner, B. Nilsson, F. Gebhard, J. D. Lambris, and M. Huber-Lang. 2010. Molecular intercommunication between the complement and coagulation systems. *J. Immunol.* 185: 5628–5636.
- Mollnes, T. E., O. L. Brekke, M. Fung, H. Fure, D. Christiansen, G. Bergseth, V. Videm, K. T. Lappégård, J. Köhl, and J. D. Lambris. 2002. Essential role of the C5a receptor in *E. coli*-induced oxidative burst and phagocytosis revealed by a novel lepirudin-based human whole blood model of inflammation. *Blood* 100: 1869–1877.
- Munthe-Fog, L., T. Hummelshøj, B. E. Hansen, C. Koch, H. O. Madsen, K. Skjødt, and P. Garred. 2007. The impact of FCN2 polymorphisms and haplotypes on the Ficolin-2 serum levels. *Scand. J. Immunol.* 65: 383–392.
- Munthe-Fog, L., T. Hummelshøj, Y. J. Ma, B. E. Hansen, C. Koch, H. O. Madsen, K. Skjødt, and P. Garred. 2008. Characterization of a polymorphism in the coding sequence of FCN3 resulting in a Ficolin-3 (Hakata antigen) deficiency state. *Mol. Immunol.* 45: 2660–2666.
- Killion, J. J., and E. M. Holtgrewe. 1983. Preparation of (Fab')₂ fragments of immunoglobulin G. *Clin. Chem.* 29: 1982–1984.
- Holmgren, A. 1979. Thioredoxin catalyzes the reduction of insulin disulfides by dithiothreitol and dihydrolipoamide. *J. Biol. Chem.* 254: 9627–9632.
- Otto, M., H. Hawlisch, P. N. Monk, M. Müller, A. Klos, C. L. Karp, and J. Köhl. 2004. C5a mutants are potent antagonists of the C5a receptor (CD88) and of C5L2: position 69 is the locus that determines agonism or antagonism. *J. Biol. Chem.* 279: 142–151.
- Heller, T., M. Hennecke, U. Baumann, J. E. Gessner, A. M. zu Vilsendorf, M. Baensch, F. Boulay, A. Kola, A. Klos, W. Bausch, and J. Köhl. 1999. Selection of a C5a receptor antagonist from phage libraries attenuating the inflammatory response in immune complex disease and ischemia/reperfusion injury. *J. Immunol.* 163: 985–994.
- Hara, T., N. Kondo, H. Nakamura, H. Okuyama, A. Mitsui, Y. Hoshino, and J. Yodoi. 2007. Cell-surface thioredoxin-1: possible involvement in thiol-mediated leukocyte-endothelial cell interaction through lipid rafts. *Antioxid. Redox Signal.* 9: 1427–1437.
- Skalska, J., P. S. Brookes, S. M. Nadochiy, S. P. Hilchey, C. T. Jordan, M. L. Guzman, S. B. Maggirwar, M. M. Briehl, and S. H. Bernstein. 2009. Modulation of cell surface protein free thiols: a potential novel mechanism of action of the sesquiterpene lactone parthenolide. *PLoS One* 4: e8115.
- Turano, C., S. Coppari, F. Altieri, and A. Ferraro. 2002. Proteins of the PDI family: unpredicted non-ER locations and functions. *J. Cell. Physiol.* 193: 154–163.
- Spitzer, D., L. M. Mitchell, J. P. Atkinson, and D. E. Hourcade. 2007. Properdin can initiate complement activation by binding specific target surfaces and providing a platform for de novo convertase assembly. *J. Immunol.* 179: 2600–2608.
- Pekkari, K., J. Avila-Cariño, R. Gurunath, A. Bengtsson, A. Schevinius, and A. Holmgren. 2003. Truncated thioredoxin (Trx80) exerts unique mitogenic cytokine effects via a mechanism independent of thiol oxidoreductase activity. *FEBS Lett.* 539: 143–148.
- Cortes-Bratti, X., E. Bassères, F. Herrera-Rodriguez, S. Botero-Kleiven, G. Coppotelli, J. B. Andersen, M. G. Masucci, A. Holmgren, E. Chaves-Olarte, T. Frisan, and J. Avila-Cariño. 2011. Thioredoxin 80-activated-monocytes (TAMs) inhibit the replication of intracellular pathogens. *PLoS One* 6: e16960.
- Fosbrink, M., F. Niculescu, V. Rus, M. L. Shin, and H. Rus. 2006. C5b-9-induced endothelial cell proliferation and migration are dependent on Akt inactivation of forkhead transcription factor FOXO1. *J. Biol. Chem.* 281: 19009–19018.
- Fischetti, F., and F. Tedesco. 2006. Cross-talk between the complement system and endothelial cells in physiologic conditions and in vascular diseases. *Autoimmunity* 39: 417–428.

35. Skeie, J. M., J. H. Fingert, S. R. Russell, E. M. Stone, and R. F. Mullins. 2010. Complement component C5a activates ICAM-1 expression on human choroidal endothelial cells. *Invest. Ophthalmol. Vis. Sci.* 51: 5336–5342.
36. Kilgore, K. S., J. P. Shen, B. F. Miller, P. A. Ward, and J. S. Warren. 1995. Enhancement by the complement membrane attack complex of tumor necrosis factor- α -induced endothelial cell expression of E-selectin and ICAM-1. *J. Immunol.* 155: 1434–1441.
37. Schroeder, B. O., Z. Wu, S. Nuding, S. Groscurth, M. Marcinowski, J. Beisner, J. Buchner, M. Schaller, E. F. Stange, and J. Wehkamp. 2011. Reduction of disulphide bonds unmasks potent antimicrobial activity of human β -defensin 1. *Nature* 469: 419–423.
38. Zoppi, M., M. Weiss, U. E. Nydegger, T. Hess, and P. J. Späth. 1990. Recurrent meningitis in a patient with congenital deficiency of the C9 component of complement: first case of C9 deficiency in Europe. *Arch. Intern. Med.* 150: 2395–2399.
39. Nakamura, T., Y. Hoshino, A. Yamada, A. Teratani, S. Furukawa, H. Okuyama, S. Ueda, H. Wada, J. Yodoi, and H. Nakamura. 2007. Recombinant human thioredoxin-1 becomes oxidized in circulation and suppresses bleomycin-induced neutrophil recruitment in the rat airway. *Free Radic. Res.* 41: 1089–1098.
40. Huber-Lang, M., V. J. Sarma, K. T. Lu, S. R. McGuire, V. A. Padgaonkar, R. F. Guo, E. M. Younkin, R. G. Kunkel, J. Ding, R. Erickson, et al. 2001. Role of C5a in multiorgan failure during sepsis. *J. Immunol.* 166: 1193–1199.
41. Nakamura, H., Y. Hoshino, H. Okuyama, Y. Matsuo, and J. Yodoi. 2009. Thioredoxin 1 delivery as new therapeutics. *Adv. Drug Deliv. Rev.* 61: 303–309.
42. Shashidharamurthy, R., R. A. Hennigar, S. Fuchs, P. Palaniswami, M. Sherman, and P. Selvaraj. 2008. Extravasations and emigration of neutrophils to the inflammatory site depend on the interaction of immune-complex with Fc γ receptors and can be effectively blocked by decoy Fc γ receptors. *Blood* 111: 894–904.
43. Heller, T., J. E. Gessner, R. E. Schmidt, A. Klos, W. Bautsch, and J. Köhl. 1999. Cutting edge: Fc receptor type I for IgG on macrophages and complement mediate the inflammatory response in immune complex peritonitis. *J. Immunol.* 162: 5657–5661.
44. Köhl, J., and J. E. Gessner. 1999. On the role of complement and Fc γ -receptors in the Arthus reaction. *Mol. Immunol.* 36: 893–903.
45. Godau, J., T. Heller, H. Hawlisch, M. Trappe, E. Howells, J. Best, J. Zwirner, J. S. Verbeek, P. M. Hogarth, C. Gerard, et al. 2004. C5a initiates the inflammatory cascade in immune complex peritonitis. *J. Immunol.* 173: 3437–3445.
46. Zhang, Y., B. F. Ramos, and B. A. Jakschik. 1991. Augmentation of reverse arthus reaction by mast cells in mice. *J. Clin. Invest.* 88: 841–846.
47. Höpken, U. E., B. Lu, N. P. Gerard, and C. Gerard. 1997. Impaired inflammatory responses in the reverse arthus reaction through genetic deletion of the C5a receptor. *J. Exp. Med.* 186: 749–756.
48. Ramos, B. F., Y. Zhang, and B. A. Jakschik. 1994. Neutrophil elicitation in the reverse passive Arthus reaction: complement-dependent and -independent mast cell involvement. *J. Immunol.* 152: 1380–1384.
49. Sjöberg, A., P. Onnerfjord, M. Mörgelin, D. Heinegård, and A. M. Blom. 2005. The extracellular matrix and inflammation: fibromodulin activates the classical pathway of complement by directly binding C1q. *J. Biol. Chem.* 280: 32301–32308.
50. Sjöberg, A. P., L. A. Trouw, and A. M. Blom. 2009. Complement activation and inhibition: a delicate balance. *Trends Immunol.* 30: 83–90.
51. Trouw, L. A., A. A. Bengtsson, K. A. Gelderman, B. Dahlbäck, G. Sturfelt, and A. M. Blom. 2007. C4b-binding protein and factor H compensate for the loss of membrane-bound complement inhibitors to protect apoptotic cells against excessive complement attack. *J. Biol. Chem.* 282: 28540–28548.
52. Lemarechal, H., P. Anract, J. L. Beaudoux, D. Bonnefont-Rousselot, O. G. Ekindjian, and D. Borderie. 2007. Expression and extracellular release of Trx80, the truncated form of thioredoxin, by TNF- α - and IL-1 β -stimulated human synoviocytes from patients with rheumatoid arthritis. *Clin. Sci.* 113: 149–155.
53. Pekkari, K., and A. Holmgren. 2004. Truncated thioredoxin: physiological functions and mechanism. *Antioxid. Redox Signal.* 6: 53–61.
54. Newman, G. W., M. K. Balcewicz-Sablinska, J. R. Guarnaccia, H. G. Remold, and D. S. Silberstein. 1994. Opposing regulatory effects of thioredoxin and eosinophil cytotoxicity-enhancing factor on the development of human immunodeficiency virus 1. *J. Exp. Med.* 180: 359–363.